Particle-in-Cell Simulations of Plasma Interaction with Lunar Crustal Magnetic Anomalies

Andrew R. Poppe[1,2], Jasper S. Halekas[1,2], Gregory T. Delory[1,2] and William M. Farrell[2,3], [1]Space Sciences Laboratory, University of California at Berkeley, Berkeley, CA, 94720, [2]NASA Lunar Science Institute, Ames Research Center, Mountain View, CA, [3]Goddard Space Flight Center, Greenbelt, MD (poppe@ssl.berkeley.edu)

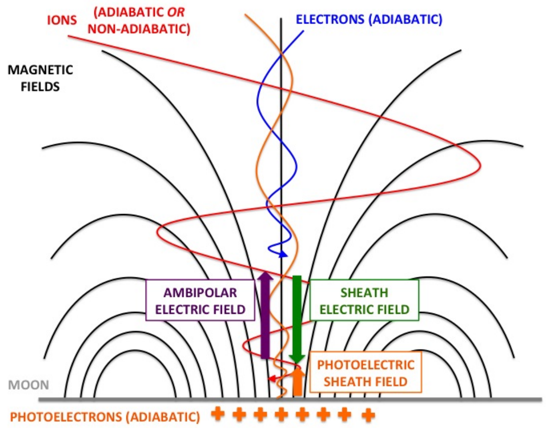

Figure 1: A cartoon depicting the various fields and particle populations present in the interaction between an ambient plasma and a lunar crustal magnetic anomaly.

Introduction

Recent observations and analysis of both lunar surface hydration and the formation of lunar swirls has stimulated the need for a quantitative understanding of the role that lunar crustal remanent magnetic fields play in shaping the near-surface lunar plasma environment [1, 2]. The lunar surface is continuously exposed to a variety of ambient plasmas which, in combination with solar UV-induced photoemission and surface remanent magnetic fields, determine the plasma environment near the lunar surface. Any acceleration and/or deceleration of protons due to near-surface electrostatic potentials or crustal remanent magnetic fields can significantly alter the proton flux to the lunar surface. In this study, we use a 1½-dimensional, electrostatic particle-in-cell code to model the self-consistent plasma environment above the lunar dayside in the presence of lunar crustal remanent magnetic fields. We discuss the implications of this work for magnetic shielding of the lunar surface, including the role that crustal fields may play in the formation of lunar swirls and proton bombardment of the lunar surface.

Particle-in-Cell Simulations

Figure 1 shows a cartoon overview of the geometry and various particle populations and fields present in this model. Shown in grey and black, respectively, are the lunar surface and a dipolar model of the lunar crustal remanent magnetic field. The simulation axis models the central field line, normal to the lunar surface. Electrons (blue) and ions (red) enter the magnetic sheath region, gyrating around the magnetic fields lines with different gyro-radii. Photoelectrons (orange) are generated at the lunar surface and are typically bound to the field lines given their small gyro-radius. In the absence of crustal magnetic fields, it has been shown that two opposing electric fields develop an equilibrium, with the sheath electric field (green) accelerating ions into the near-surface region and the photoelectric field (orange) trapping photoelectrons near the surface [3]. Introducing a magnetic field to the model should generate an ambipolar electric field (purple) due to the non-adiabatic nature of the ions. The sheath and ambipolar electric fields should oppose each other, yet will not necessarily have identical strength as a function of height above the surface.

In order to simulate the effect of crustal remanent magnetic fields on the lunar photoelectron sheath, we use a 1½-dimensional, electrostatic particle-in-cell (PIC) code, adapted from a 1-dimensional PIC code previously used to model this environment [3, 4, 5]. The 1½-d code is identical to the 1-d code, with the addition that perpendicular velocities are now tracked for all particles. Our initial modeling has used a relatively simple geometry for the magnetic fields due to the low dimensionality of the 1½-d code, namely, a magnetic mirror, where the magnetic field and the simulation axis are aligned. The magnetic field, $B(z)$, is comprised of two components: the background magnetic field, B_{bg}, assumed to be a constant throughout the simulation, and the crustal anomaly field, $B_{anom}(z)$, which varies along the simulation axis. Similar to previous work, we model the crustal anomaly field to be due to a magnetic dipole with moment, m_o, buried at some depth, h, below the lunar surface [7]; however, we only consider the case where the dipole is aligned with the simulation axis, due to the 1½-d nature of the simulation. The strength of the anomaly magnetic field then has the form, $B_{anom}(z) \propto (z+h)^{-3}$, with derivative $dB_z(z)/dz \propto (z+h)^{-4}$, which generates the well-known magnetic mirror restoring force, $F(z) = -\mu dB_z(z)/dz$, where $\mu = \frac{1}{2}mv_\perp^2/B$ is the magnetic moment of the particle. As particles enter the simulation at either end, they are assigned parallel and

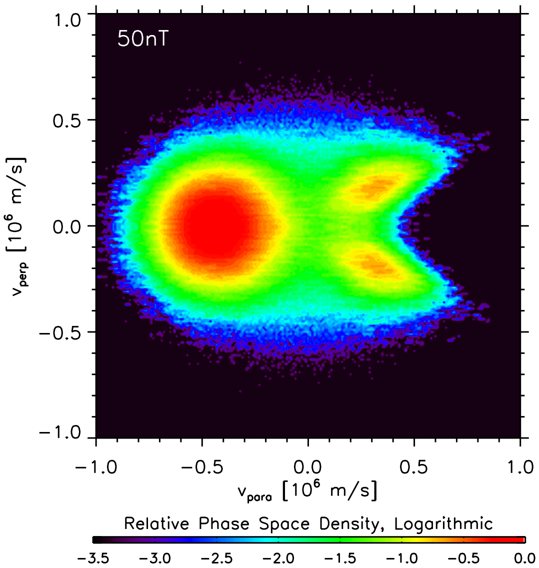

Figure 2: The logarithmic, relative phase space density of solar wind protons above a 50nT crustal surface magnetic field.

perpendicular velocities according to specified distributions. Using the initial perpendicular velocity and the local value of the magnetic field, the magnetic moment for each particle can be calculated. Under the adiabatic assumption, $d\mu/dt = 0$, and thus, we can use the conservation of μ to calculate the perpendicular velocity at any later point in time by using the strength of the magnetic field at the particles location. Parallel velocities are then subject to the sum of the electrostatic and magnetic mirror forces,

$$m\frac{dv_{||}}{dt} = -q\nabla\phi(z) - \mu\frac{dB_z(z)}{dz}. \quad (1)$$

It is important to note that while the electric force depends on the charge of the particle, q, the magnetic mirror force does not, and for all magnetic field models used here, always points away from the surface for both ions and electrons.

Preliminary Results

Initial simulations have focused on modeling two basic incoming plasma distributions: (1) the terrestrial plasma sheet, where the plasma has typical temperatures of 100-1000 eV with no bulk drift, and (2) the solar wind, with temperatures approximately 10 eV and a bulk drift of approximately 400 km/sec. Both simulations have been benchmarked to previous simulations without the presence of a magnetic field, in order to ensure proper functioning of the code. Following this step, we have introduced crustal magnetic fields and analyzed how variations in plasma temperature, plasma bulk speed (for the solar wind), ion anisotropy/adiabaticity and magnetic field strength and vertical structure influence the electrostatic field and particle populations, the surface charge, and the proton flux to the lunar surface. Figure 2 shows the logarithmic, relative phase space density for adiabatic solar wind protons interacting with a 50 nT crustal remanent magnetic field. The incident proton beam ($v_{||} < 0$) is partially reflected by the combined electrostatic and magnetic fields near the surface, developing an energy-dependent loss cone of protons ($v_{||} > 0$) moving away from the Moon.

We present model-predicted proton fluxes to the lunar surface as a function of plasma parameters and magnetic field strength and structure, and discuss the implications of these results for physical phenomena on the Moon, including space weathering, proton implantation and the formation of lunar swirls. Additionally, we also aim to compare this model with in-situ measurements made by the twin ARTEMIS spacecraft, currently in orbit around the Moon.

References

[1] G. Y. Kramer, et al. Characterization of lunar swirls at Mare Ingenii: A model for space weathering at magnetic anomalies. J. Geophys. Res., 116(E04008), 2011. [2] G. Y. Kramer, et al. M^3 spectral analysis of lunar swirls and the link between optical maturation and surface hydroxyl formation at magnetic anomalies. J. Geophys. Res., 116(E00G18), 2011. [3] A. Poppe and M. Horányi. Simulations of the Photoelectron Sheath and Dust Levitation on the Lunar Surface. J. Geophys. Res., 115(A08106), 2010. [4] C. K. Birdsall and A. B. Langdon. Plasma physics via computer simulation. McGraw-Hill, New York, 1985. [5] A. R. Poppe, et al. A comparison of ARTEMIS observations and particle-in-cell modeling of the lunar photoelectron sheath in the terrestrial magnetotail. Geophys. Res. Lett., 39(L01102), 2012. [6] B. Feuerbacher, et al. Photoemission from lunar surface fines and the lunar photoelectron sheath. Proc. 3rd Lunar Sci. Conf., 3:2655–2663, 1972. [7] L. L. Hood and C. R. Williams. The Lunar Swirls: Distribution and Possible Origins. Proc. 19th Lunar Sci. Conf., 19: 99–113, 1989.